AD NUMBER

AD822880

LIMITATION CHANGES

TO:

Approved for public release; distribution is unlimited.

FROM:

**Distribution authorized to U.S. Gov't. agencies and their contractors;
Administrative/Operational Use; NOV 1967. Other requests shall be referred to Arnold Engineering Development Center, Arnold AFB, TN.**

AUTHORITY

AEDC ltr 21 Oct 1974

AEDC-TR-67-224

DRAG AND PERFORMANCE CHARACTERISTICS OF FLEXIBLE SUPERSONIC DECELERATOR MODELS AT MACH NUMBERS FROM 2 TO 6

A. W. Myers

ARO, Inc.

November 1967

VON KÁRMÁN GAS DYNAMICS FACILITY
ARNOLD ENGINEERING DEVELOPMENT CENTER
AIR FORCE SYSTEMS COMMAND
ARNOLD AIR FORCE STATION, TENNESSEE

NOTICES

When U. S. Government drawings specifications, or other data are used for any purpose other than a definitely related Government procurement operation, the Government thereby incurs no responsibility nor any obligation whatsoever, and the fact that the Government may have formulated, furnished, or in any way supplied the said drawings. specifications, or other data, is not to be regarded by implication or otherwise, or in any manner licensing the holder or any other person or corporation, or conveying any rights or permission to manufacture, use, or sell any patented invention that may in any way be related thereto.

Qualified users may obtain copies of this report from the Defense Documentation Center.

References to named commercial products in this report are not to be considered in any sense as an endorsement of the product by the United States Air Force or the Government.

DRAG AND PERFORMANCE CHARACTERISTICS OF FLEXIBLE SUPERSONIC DECELERATOR MODELS AT MACH NUMBERS FROM 2 TO 6

A. W. Myers
ARO, Inc.

AF – AEDC
Arnold AFS Tenn

FOREWORD

The work reported herein was done at the request of the Air Force Flight Dynamics Laboratory (AFFDL) (FDFR), Air Force Systems Command (AFSC), under Program Element 6240533F, Project 6065, Task 606507.

The results of tests presented were obtained by ARO, Inc. (a subsidiary of Sverdrup & Parcel and Associates, Inc.), contract operator of the Arnold Engineering Development Center (AEDC), AFSC, Arnold Air Force Station, Tennessee, under Contract AF40(600)-1200. This report presents data, not previously published, obtained during the course of a continuing test program initiated in February 1966 under ARO Project No. VT0626. The manuscript was submitted for publication on September 28, 1967.

This technical report has been reviewed and is approved.

Donald H. Meyer
Major, USAF
AF Representative, VKF
Directorate of Test

Leonard T. Glaser
Colonel, USAF
Director of Test

ABSTRACT

The drag and stability characteristics of flexible supersonic decelerator models at various positions aft of double-strut mounted forebodies were investigated in the 40-in. supersonic tunnel of the von Kármán Gas Dynamics Facility. Data were obtained at Mach numbers from 2 to 6 at dynamic pressures corresponding to pressure altitudes which ranged from 94,000 to 153,000 ft. Selected typical results are presented.

CONTENTS

		Page
	ABSTRACT	iii
	NOMENCLATURE	vi
I.	INTRODUCTION	1
II.	APPARATUS	
	2.1 Wind Tunnel	1
	2.2 Test Articles	1
	2.3 Instrumentation	2
III.	TEST PROCEDURE	3
IV.	RESULTS AND DISCUSSION	
	4.1 Parachute Drag	3
	4.2 Parachute Performance	4
	REFERENCES	5

APPENDIXES

I. ILLUSTRATIONS

Figure

1. Forebody and Strut Details
   - a. Forebody Details . . . 9
   - b. Strut Details . . . 10
   - c. Tunnel Installation Sketch . . . 10
2. Parachute Design and Construction Details
   - a. Parachute Construction and Profile Details . . . 11
   - b. Configuration 1 in Tunnel A, M_∞ = 3, q_∞ = 1.0 psia . . . 12
   - c. Configuration Photographs . . . 12
3. Effects of Forebody Shape and Canopy x/d Location on the Parachute Drag Coefficient, Parachute Configuration 2, q_∞ = 1.0 psia . . . 13
4. Effect of Parachute Trailing Distance on the Forebody Wake and Canopy Inflation Characteristics, Forebody Configuration 3, Parachute Configuration 2, M_∞ = 6, q_∞ = 1.0 psia . . . 14

Figure | Page

5. Comparison of C_{D_p} for Parachute Configurations 1 and 2, Forebody 1, q_∞ = 1.0 psia 15
6. Variation of Drag Coefficient with Mach Number, Parachute Configuration 2, q_∞ = 1.0 psia 16
7. Effects of Parachute Trailing Distance on Forebody Base Pressure, Forebody Configuration 1, Parachute Configuration 2, q_∞ = 1.0 psia 17

II. TABLE

I. Summary of Parachute Test Conditions and Performance Results 18

NOMENCLATURE

C_{D_p}	Drag coefficient of parachute canopy based on projected canopy area, drag force/$q_\infty S_p$
d	Forebody base diameter, in.
M_∞	Free-stream Mach number
p_b	Forebody base pressure, psia
p_∞	Free-stream static pressure, psia
q_∞	Free-stream dynamic pressure, psia
S_p	Design projected area of inflated parachute canopy, $in.^2$
x	Distance from the base of the forebody model to the parachute canopy inlet, in.
λ	Parachute canopy geometric porosity, percent

SECTION I
INTRODUCTION

Tests were conducted in the Gas Dynamic Wind Tunnel, Supersonic (A), of the von Kármán Gas Dynamics Facility (VKF), to determine the drag and stability characteristics of flexible supersonic decelerator models at various positions aft of several double-strut mounted forebodies. The decelerator canopy designs were experimental, and the forebodies included both axisymmetric and asymmetric configurations. The tests were conducted in support of the EUREKA (Establishment of an Unsymmetrical Wake Test Capability for Aerodynamic Decelerators) program at Mach numbers from 2 to 6, at dynamic pressures corresponding to pressure altitudes which ranged from 94,000 to 153,000 ft.

Selected typical results are presented showing the effects of Mach number, location in the wake, and design parameters on the parachute drag. The parachute performance and stability (stability as discussed in this report refers only to the conditions of oscillatory motion of the parachute with respect to the forebody model) are summarized for each test condition in Table I, Appendix II.

SECTION II
APPARATUS

2.1 WIND TUNNEL

Tunnel A is a continuous, closed-circuit, variable density wind tunnel with an automatically driven, flexible-plate-type nozzle and a 40- by 40-in. test section. The tunnel operates at Mach numbers from 1.5 to 6 at maximum stagnation pressures from 29 to 200 psia, respectively, and stagnation temperatures up to 300°F (M_∞ = 6). Minimum operating pressures range from about one-tenth to one-twentieth of the maximum pressures. A description of the tunnel and airflow calibration information may be found in Ref. 1.

2.2 TEST ARTICLES

2.2.1 Forebody Models and Support System

The three models employed as forebodies during the tests were a sharp cone-cylinder (Configuration 1), a 0.182-scale model of the basic

Arapaho "C" test vehicle consisting of a blunt cone-cylinder-flare (Configuration 2), and a blunted elliptical cone (Configuration 3). Details of the forebody configurations are shown in Fig. 1a.

The forebody support system (Fig. 1b) consisted of a strut spanning the width of the tunnel and mounted to the sidewalls. The drag tensiometer and a winch assembly for varying the location of the decelerator aft of the forebody were housed in a vacuum tank which was also mounted to the tunnel sidewall (Fig. 1b). The decelerator support line passed through the model and strut and into the vacuum tank where it was attached to the tensiometer and winch assembly.

2.2.2 Decelerator Models

The parachutes were designed and constructed by AFFDL, and details are shown in Fig. 2. They were constructed of solid, relatively nonporous, cloth with a single exit opening which controlled the airflow through the canopy. Configuration 1 was constructed with surface contours determined from shallow water tow tests using the gas-hydraulic analogy, and Configuration 2 was constructed in the shape Configuration 1 assumed when inflated in supersonic flow. That is, the surface contours for Configuration 2 were determined from test photographs taken of Configuration 1 parachutes during an earlier test entry. Total geometric porosity, based on the entrance and exit areas, was 14 percent.

2.3 INSTRUMENTATION

Parachute drag measurements were made with a 60-lb tensiometer located in the winch assembly. A time history of the dynamic drag output from the tensiometer was recorded on an oscillograph, and average drag values were measured on a low response servopotentiometer. Based on the repeatability of the calibration results, the accuracy of the drag measurements is estimated to be within 4 percent.

Parachute performance was monitored with two high-speed, 16-mm, motion-picture cameras (one for side motion pictures and one for schlieren photography), and additional photographic results were obtained with still cameras mounted in the schlieren system and next to the test section windows.

SECTION III
TEST PROCEDURE

Before each test run, the parachute canopy and suspension lines were packed in a deployment bag which was then suspended near the base of the forebody model by a pull cord routed from the rear of the bag through the tunnel sector. The pull cord was held taut during tunnel start, and when the desired test conditions were established, a sharp pull on the cord removed the bag. Parachute location behind the forebody was set by the remotely operated winch assembly using reference marks placed on the tunnel windows.

A summary of the test conditions and decelerator performance results is given in Table I. The observations presented in the table are the results of evaluations of the photographic data.

SECTION IV
RESULTS AND DISCUSSION

4.1 PARACHUTE DRAG

The effects of forebody shape and canopy trailing distance on parachute Configuration 2 drag coefficients are presented in Fig. 3. Generally, the largest variations in drag coefficient with x/d were obtained when the parachutes were close to the forebody base ($x/d < 5$). In this region, the presence of the parachutes caused the wake to open for all forebody configurations at $M_\infty > 4$, and the parachutes behind forebody Configuration 3 were generally poorly inflated at all Mach numbers at $x/d = 3$. Visual evidence of these two effects is presented in Fig. 4.

Also presented in Fig. 3 is a comparison of the drag coefficients of parachutes in the present tests to the hyperflo parachute configuration reported in Ref. 2. The present canopy design appears to be more efficient (higher C_{D_p}) especially for $M_\infty < 4$.

Drag coefficients for the two canopy shapes behind forebody Configuration 1 are compared in Fig. 5, and it can be seen that the larger canopy design of parachute Configuration 2 yielded the higher drag value at all test conditions.

The decrease in parachute drag coefficient with Mach number is shown in Fig. 6 for a range of x/d values. The closed symbols in Fig. 6 represent drag coefficients calculated for a disk with an area equal to the projected area less the exit area of the parachutes tested. Frontal pressures on the disk were assumed to be constant and equal in value to the wake centerline pitot pressure. Base pressures were calculated assuming the ratio of disk base pressure to wake centerline static pressure was the same as forebody base pressure to free-stream static pressure. Also included in the figure (flagged solid symbols) are the results for x/d = 7 assuming zero base pressure. The wake pitot and static pressures were obtained from the wake survey data reported in Ref. 3. Good agreement was found between this simple prediction method and the measured drag coefficients of the parachutes behind forebody 2.

The variation of forebody base pressure with parachute trailing distance is shown in Fig. 7 where the base pressure is presented as a function of the difference between the base pressure with the chute at any value of x/d and the value for the chute at x/d = 10. Little or no variation was present for the x/d range covered for $M_\infty < 4$, but for $M_\infty = 5$ and 6 a large base pressure increase, associated with the opening of the forebody wake, occurred as the trailing distance was varied from x/d = 10 to x/d = 6. A decrease in parachute drag was obtained for the open wake condition as can be seen for this parachute and forebody combination in Fig. 3.

4.2 PARACHUTE PERFORMANCE

The parachute performance for each test run is presented in Table I. The parachutes were generally stable (oscillations less than 5 deg) or very stable (oscillations less than 2 deg); however, unstable conditions were noted at $M_\infty = 4$ for large trailing distances behind forebody Configuration 1.

Canopy inflation was good at all trailing distances behind the axisymmetric forebodies (1 and 2), and the inflation of canopies behind the asymmetric forebody (3) was good except at the small trailing distances (x/d < 4).

Sporadic pulsing of the canopy occurred throughout the range of test conditions behind all forebodies. This effect, however, was generally greater for the high Mach numbers and larger trailing distances.

REFERENCES

1. Test Facilities Handbook (6th Edition). "von Kármán Gas Dynamics Facility, Vol. 4." Arnold Engineering Development Center, November 1966.

2. Deitering, J. S. and Hilliard, E. E. "Wind Tunnel Investigation of Flexible Aerodynamic Decelerator Characteristics at Mach Numbers 1.5 to 6." AEDC-TR-65-110 (AD464786), June 1965.

3. Sims, Leland W. "The Effects of Design Parameters and Local Flow Fields on the Performance of Hyperflo Supersonic Parachutes and High Dynamic Pressure Parachute Concepts." AFFDL-TR-65-150, Vol. II, October 1965.

APPENDIXES

I. ILLUSTRATIONS
II. TABLE

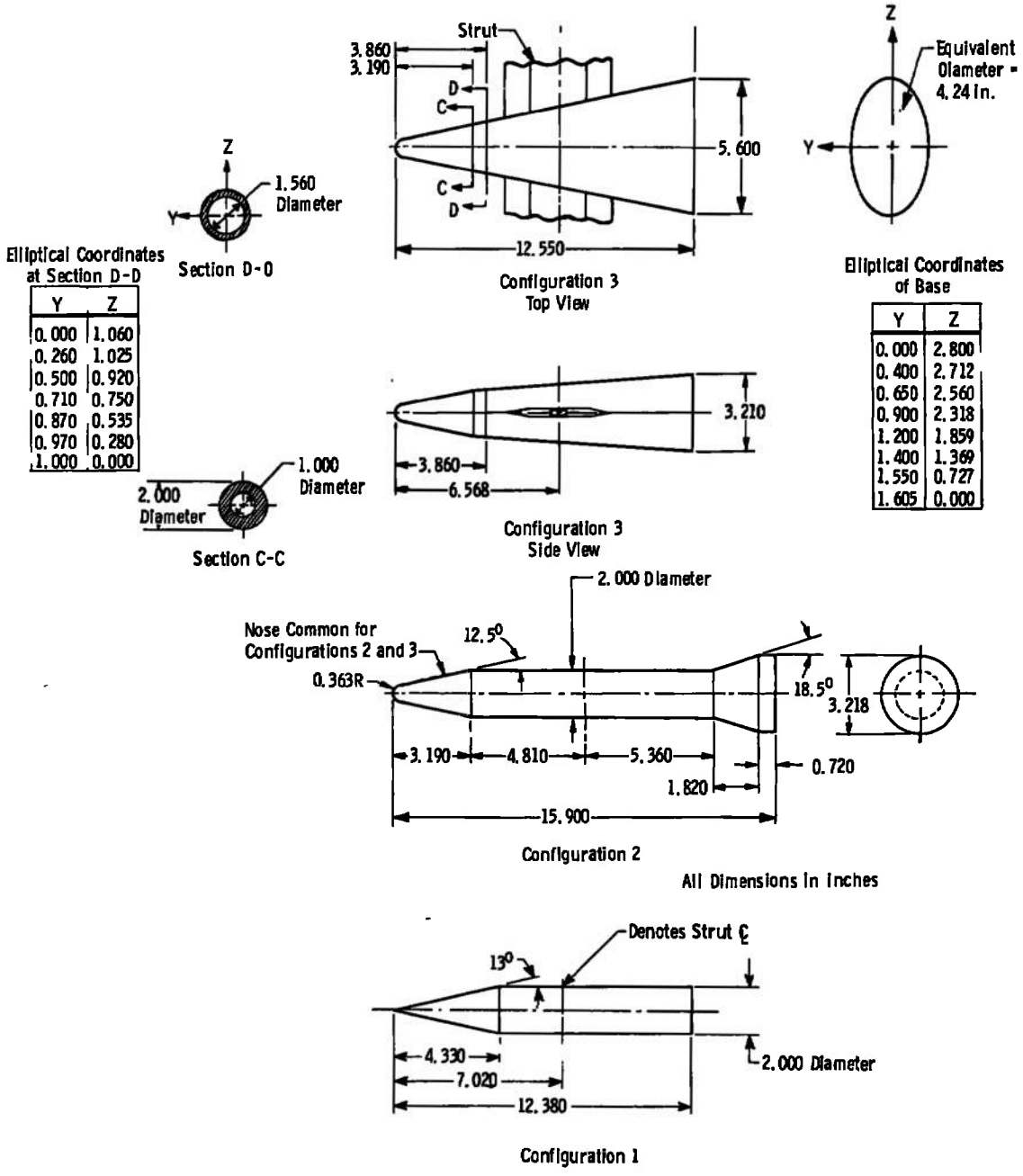

a. Forebody Details

Fig. 1 Forebody and Strut Details

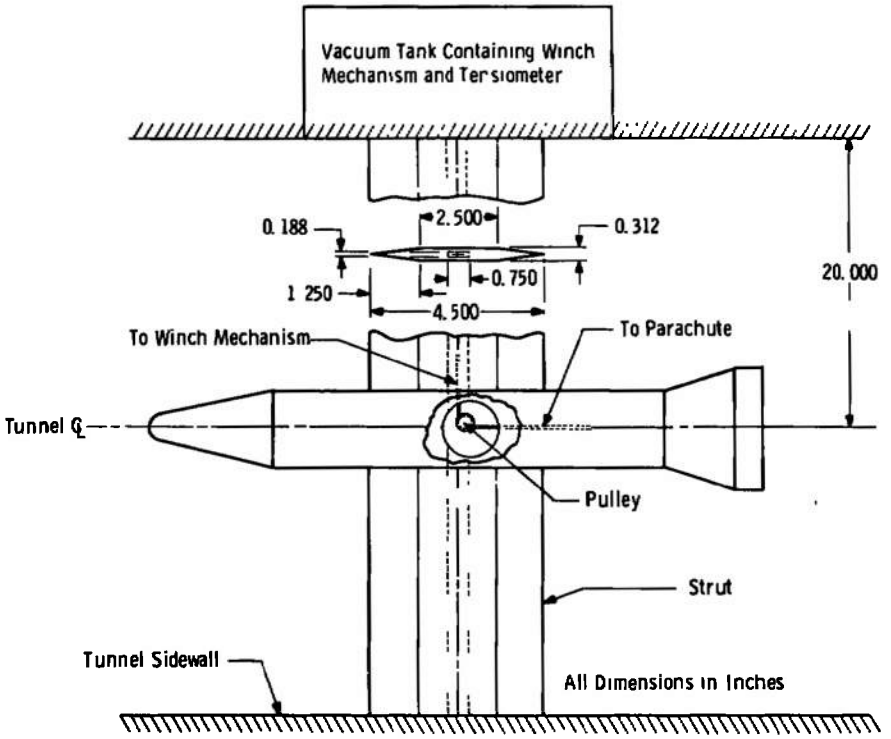

b. Strut Details

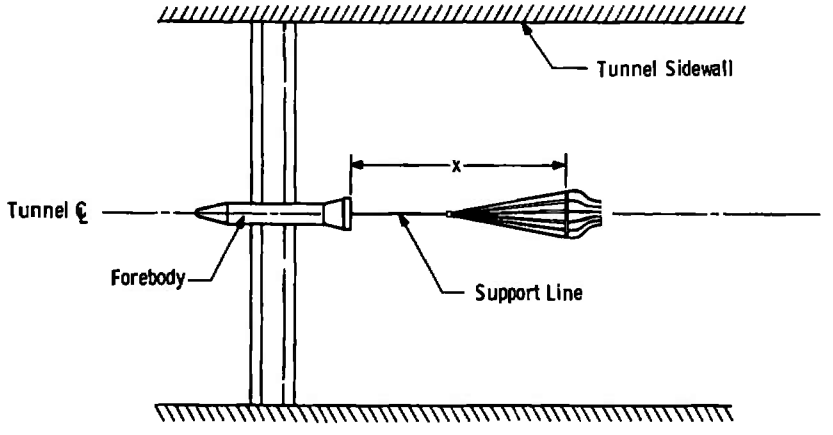

c. Tunnel Installation Sketch

Fig. 1 Concluded

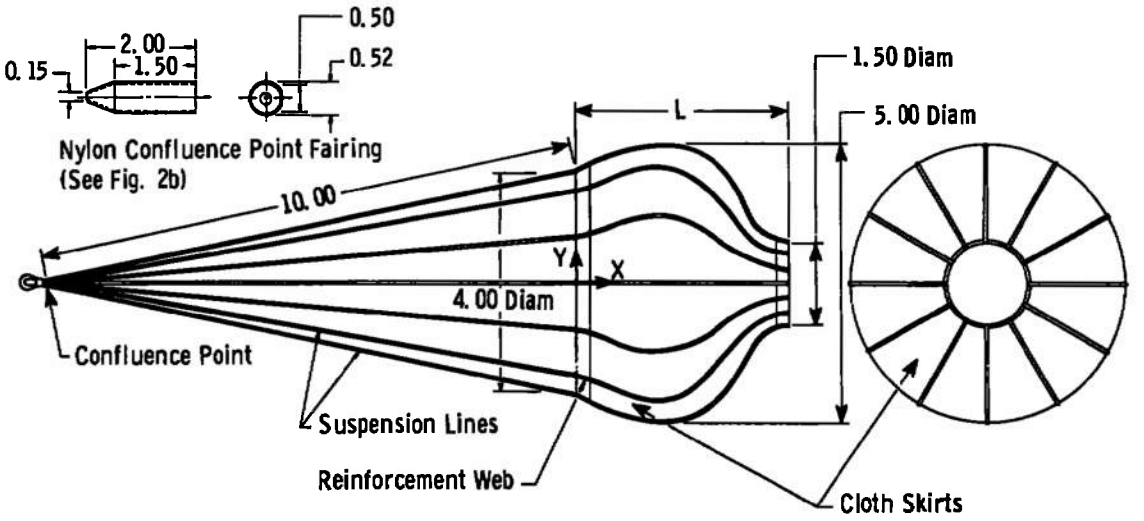

Canopy Profile Coordinates

Configuration 1		Configuration 2	
X	Y	X	Y
0	2.000	0	2.000
1.00	2.500	0.25	2.105
1.25	2.495	0.50	2.205
1.50	2.425	0.75	2.290
1.75	2.250	1.00	2.370
2.00	1.950	1.25	2.438
2.25	1.500	1.50	2.483
2.50	1.000	1.68	2.500
2.75	0.800	1.75	2.495
L = 3.00	0.750	2.00	2.435
		2.25	2.338
		2.50	2.183
		2.75	1.938
		3.00	1.535
		3.25	1.070
		3.50	0.840
		3.75	0.763
		L = 3.88	0.750

Material Specifications

Skirt Cloth - MIL-C-8021B, Type I, 200 lb

Suspension Lines - MIL-C-5040 B, Type I, 100 lb

Reinforcement Webs - MIL-T-5038 C, Type III, 400 lb

Geometric Porosity, λ, = $\left(\frac{1.5}{4.0}\right)^2$ = 14 percent

All Dimensions in Inches

a. Parachute Construction and Profile Details

Fig. 2 Parachute Design and Construction Details

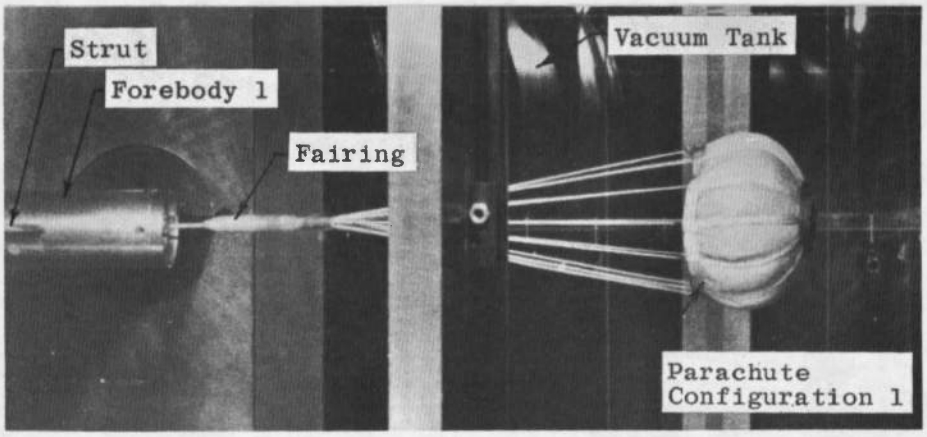

b. Configuration 1 in Tunnel A, $M_\infty = 3$, $q_\infty = 1.0$ psia

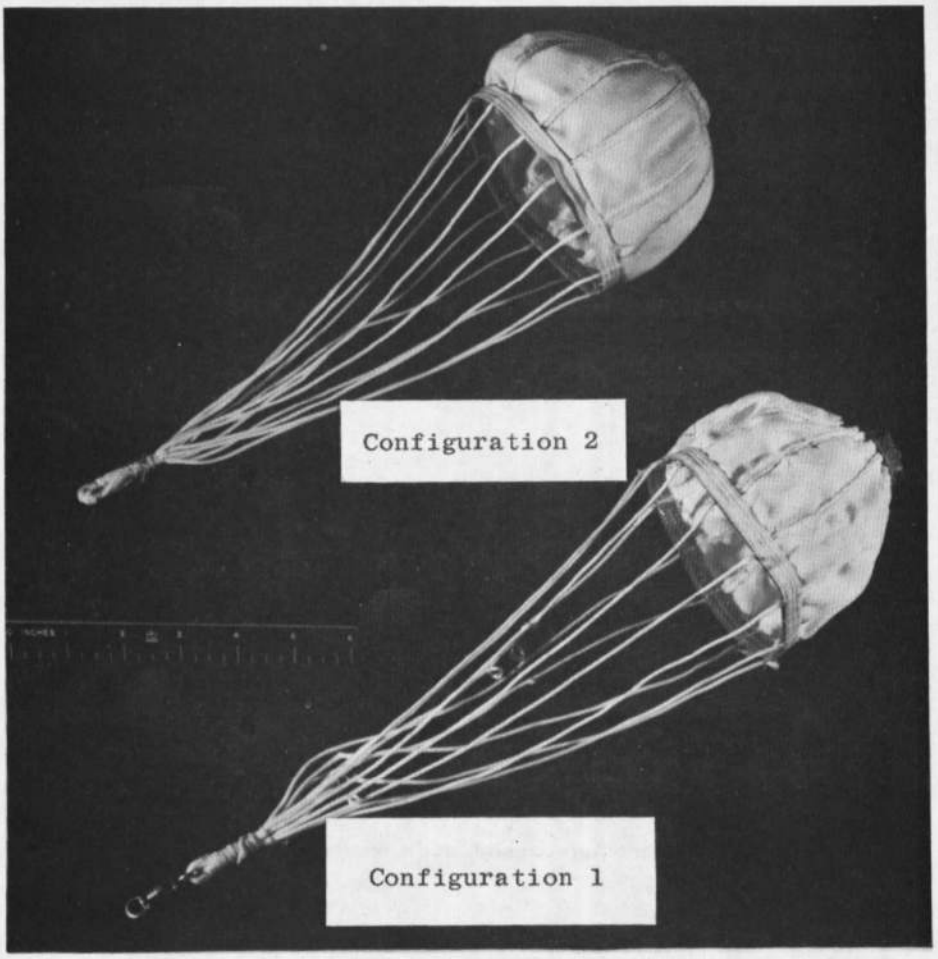

c. Configuration Photographs

Fig. 2 Concluded

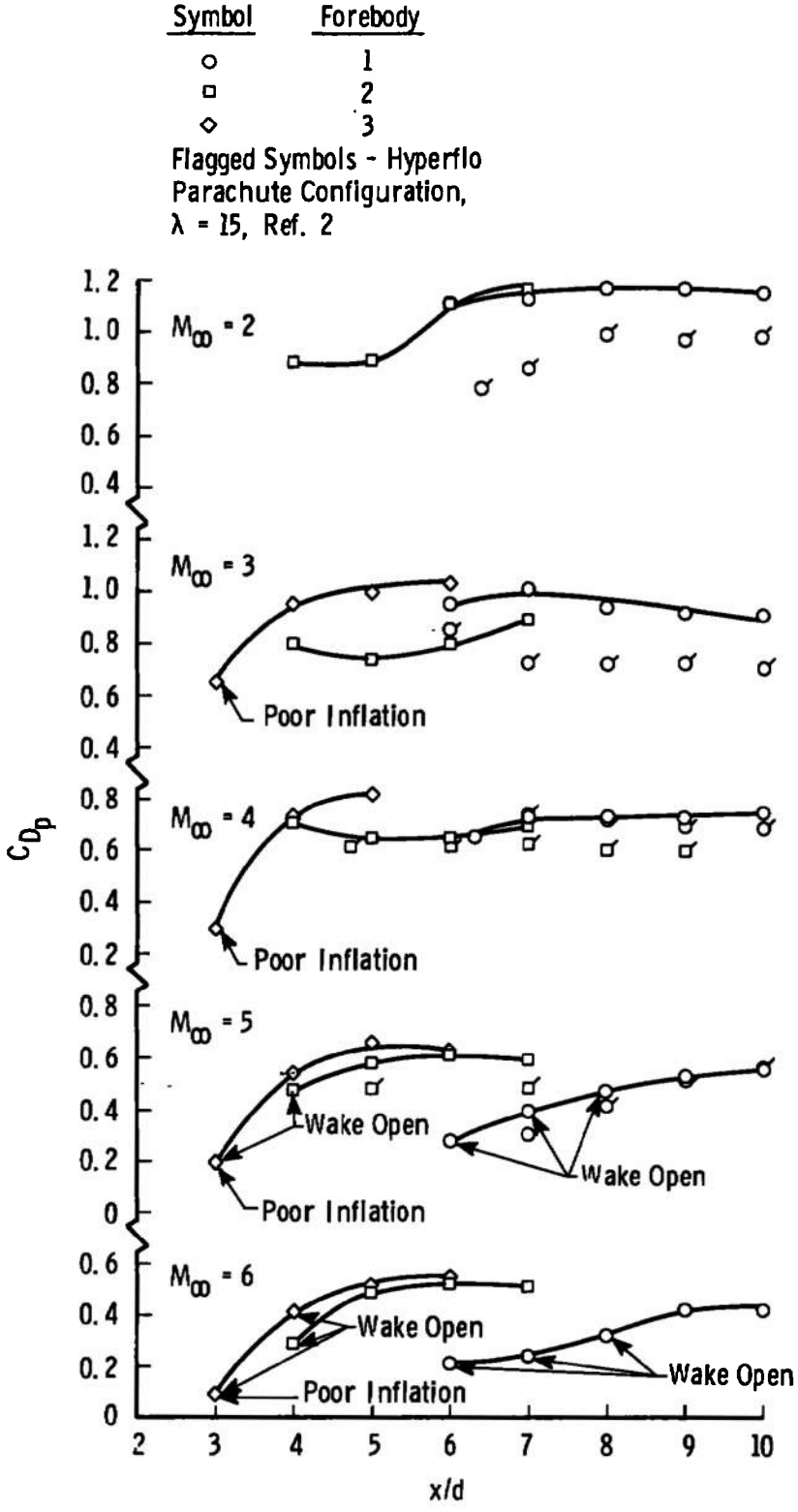

Fig. 3 Effects of Forebody Shape and Canopy x/d Location on the Porachute Drag Coefficient, Parachute Configuration 2, q_∞ = 1.0 psia

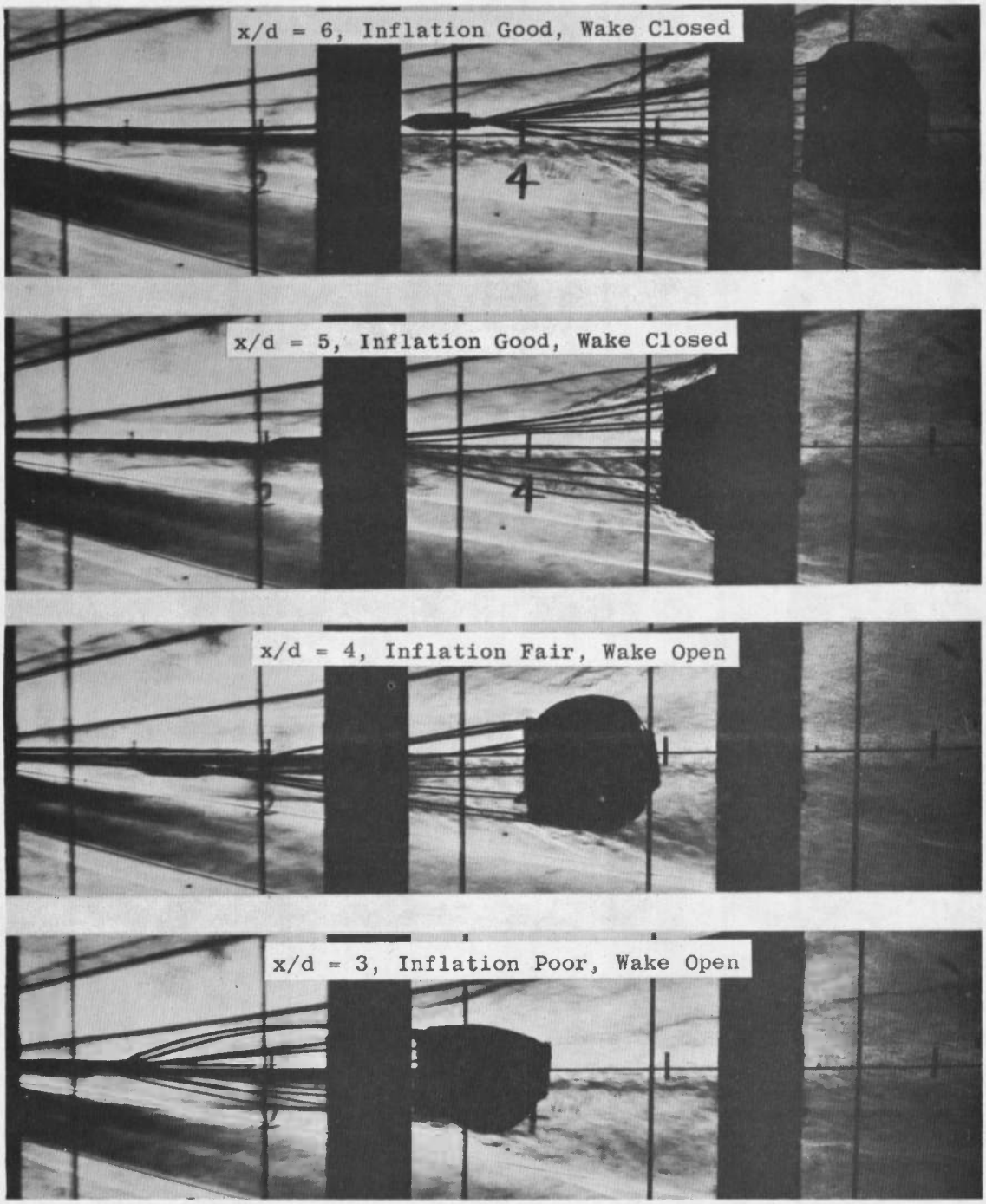

Fig. 4 Effect of Porachute Troiling Distonce on the Farebody Wake and Canopy Inflotion Charocteristics, Forebody Canfigurotion 3, Parachute Canfigurotion 2, $M_\infty = 6$, $q_\infty = 1.0$ psia

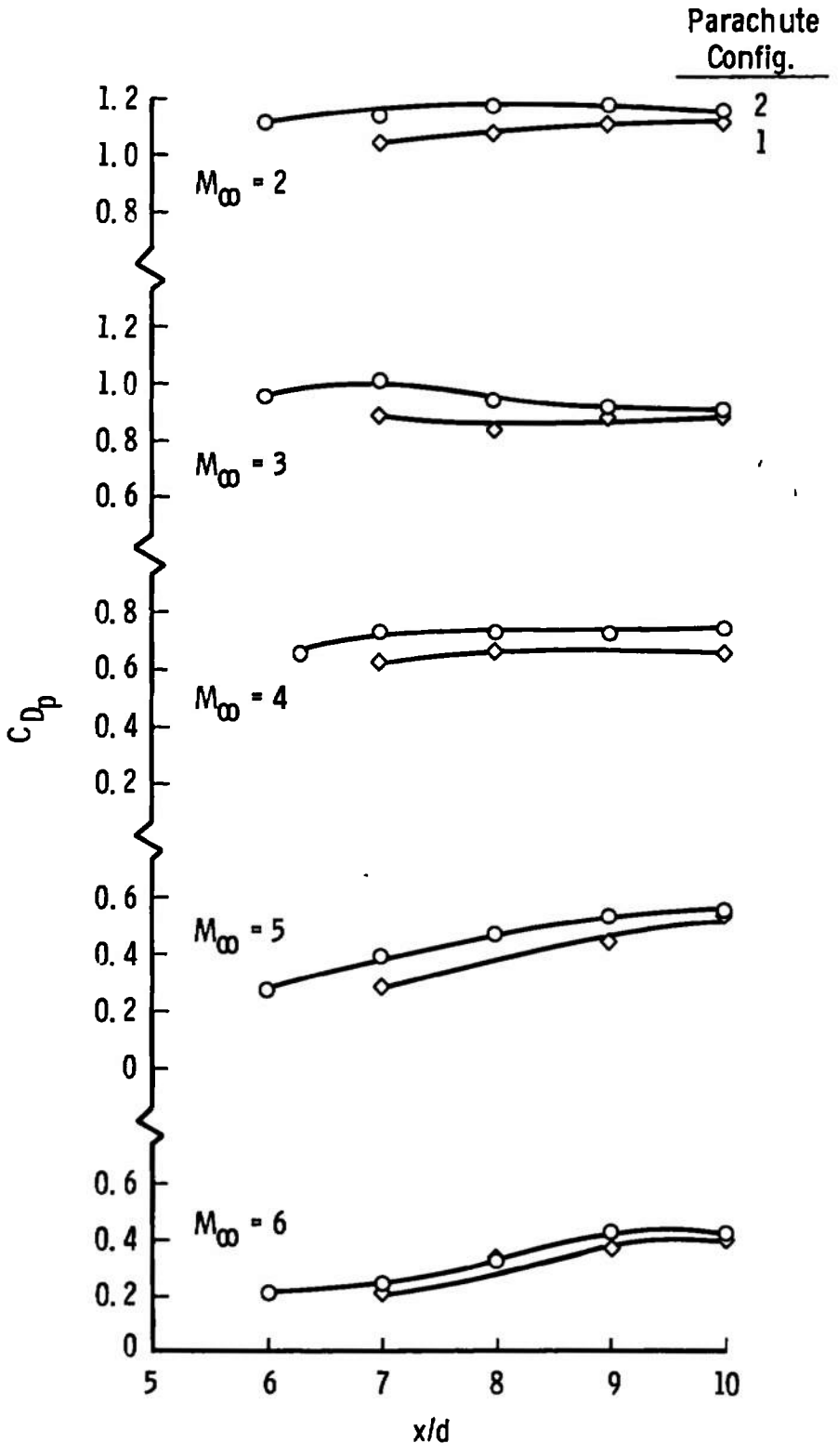

Fig. 5 Comparison of C_{D_P} for Parachute Configurations 1 and 2, Forebody 1, q_∞ = 1.0 psia

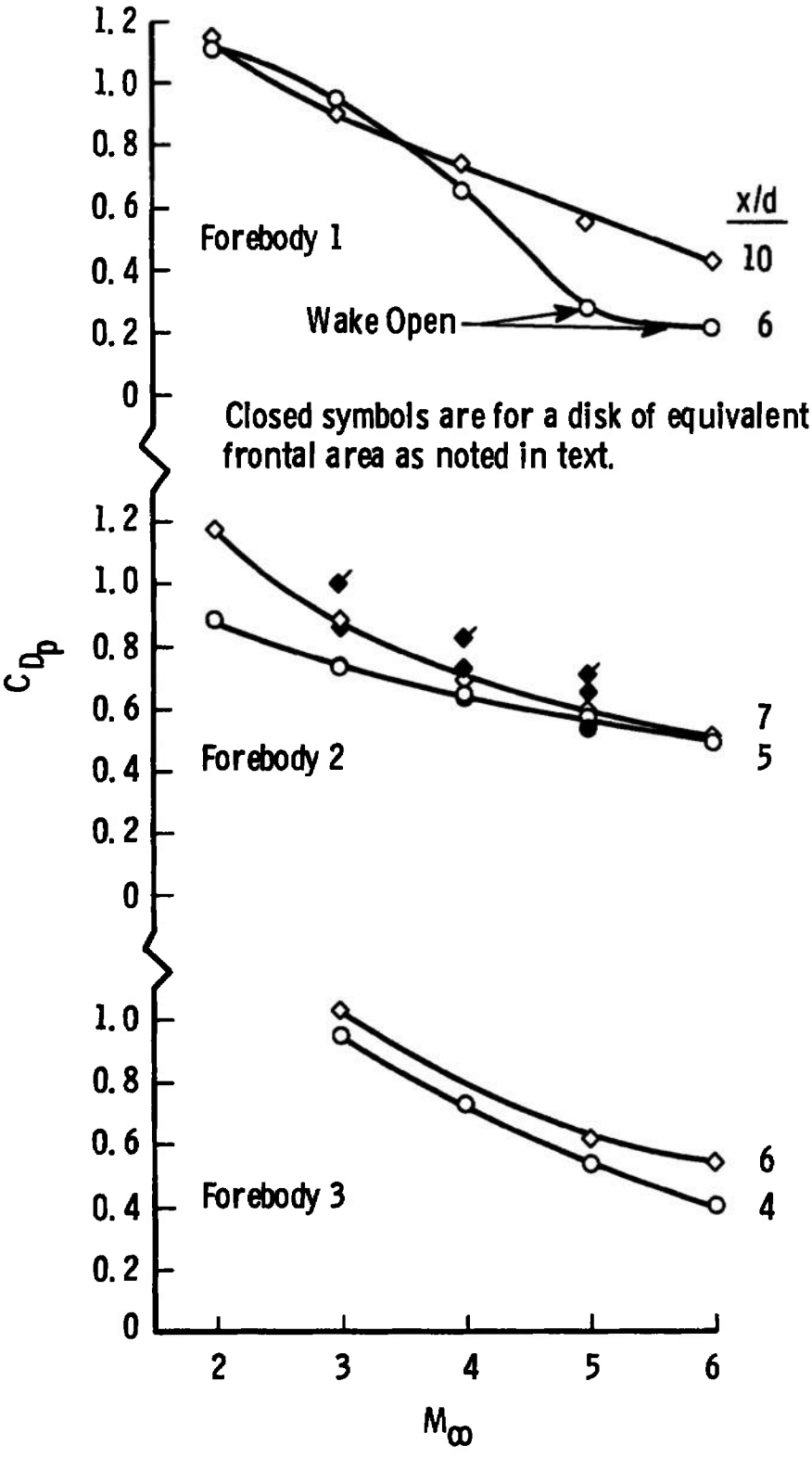

Fig. 6 Variation of Drag Coefficient with Mach Number, Parachute Configuration 2, q_∞ = 1.0 psia

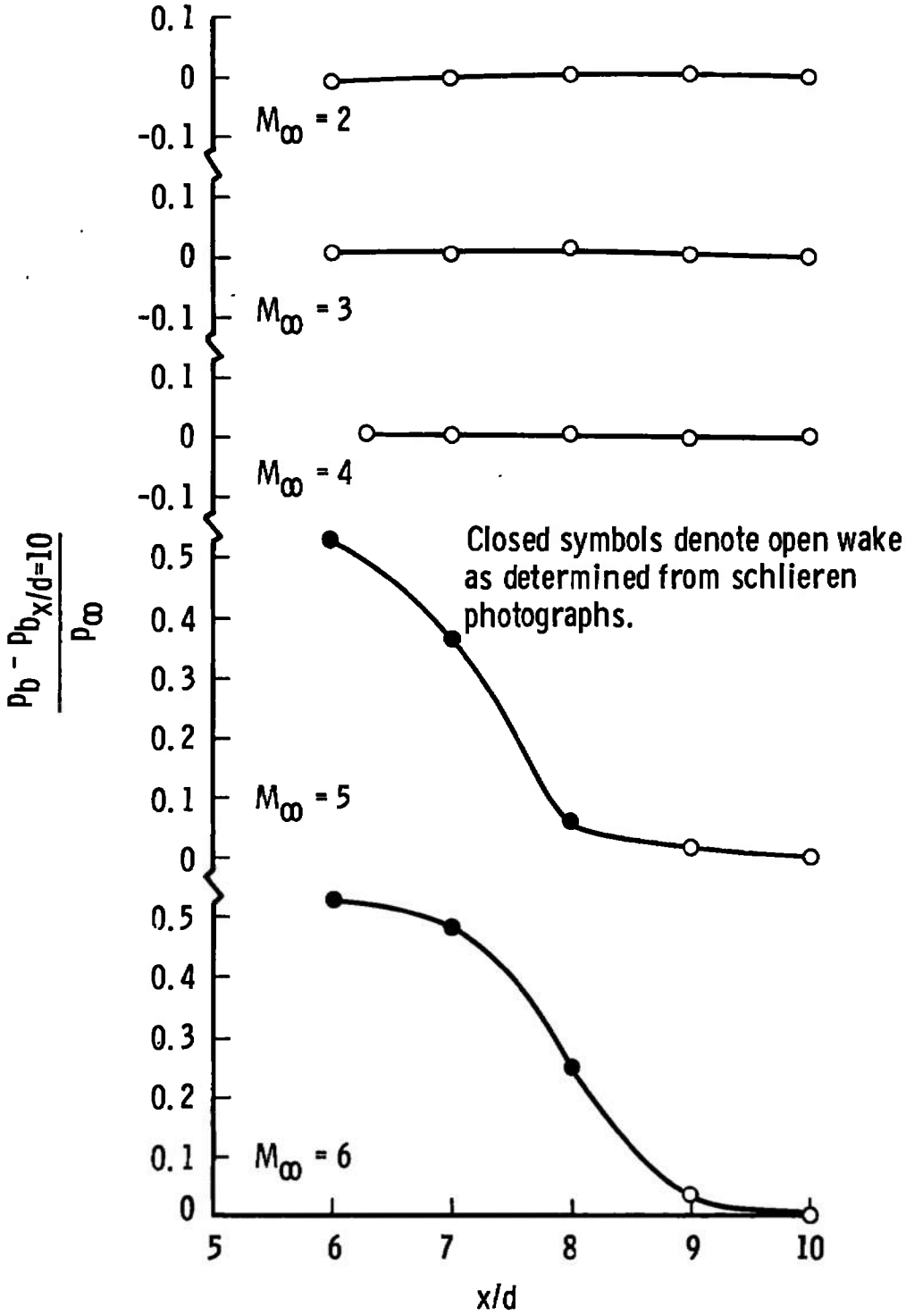

Fig. 7 Effects of Parachute Trailing Distance on Forebody Base Pressure, Forebody Configuration 1, Parachute Configuration 2, q_∞ = 1.0 psia

TABLE I
SUMMARY OF PARACHUTE TEST CONDITIONS AND PERFORMANCE RESULTS

Parachute Config.	Forebody Config.	M_∞ (Nominal)	x/d		q_∞, psia	C_{D_p}		Remarks
			Min.	Max.		Min.	Max.	
1	1	2.0	7	10	1.0	0.95	1.04	Very stable and well inflated at all x/d values. Light canopy pulsing for x/d < 9. Slowly rolling back and forth for x/d > 9.
		3.0				0.75	0.82	Stable (x/d = 10) to very stable (x/d ≤ 9). Well inflated at all x/d values. Light canopy pulsing at x/d = 7 and 8, increasing to medium to heavy pulsing for x/d > 8.
		4.0				0.62	0.82	Very stable at x/d = 7. Stable to unstable (±6 deg oscillations) for x/d > 7. Canopy pulsing increasing from light (x/d = 7) to medium and heavy (x/d > 7).
		5.0				0.28	0.53	Very stable (x/d < 8) to stable (x/d > 8). Light to medium canopy pulsing for x/d = 9 and 10. Good inflation at all x/d values.
		6.0				0.23	0.39	Same as M_∞ = 5.0
2	1	2.0	6	10	1.0	1.06	1.18	Very stable, well inflated at all x/d values. Little or no canopy pulsing.
		2.5				1.02	1.10	Same as M_∞ = 2.0 exeept light canopy pulsing at x/d = 6 and 7.
		3.0				0.90	1.01	Same as M_∞ = 2.0 except light canopy pulsing at all x/d values
		3.5	6	9		0.79	0.86	Very stable to stable and well inflated at all x/d values. Light canopy pulsing increasing to medium at x/d = 9.

Note: The following nomenclature is used in discussing parachute stability:
Very Stable - Oscillations less than ±2 deg
Stable - Oscillations between ±2 and ±5 deg
Unstable - Oscillations greater than ±5 deg

TABLE I (Continued)

Parachute Config.	Forebody Config.	M_∞ (Nominal)	x/d		q_∞, psia	C_{D_p}		Remarks
			Min.	Max.		Min.	Max.	
2	1	4.0	6.3	10	0.5	0.52	0.66	Very stable and well inflated at all x/d values. Light canopy pulsing at x/d = 9 and 10.
					1.0	0.64	0.74	Same as q_∞ = 0.5 psia except light canopy pulsing at all x/d values.
			6.3	9	1.5	0.61	0.74	Very stable, well inflated, with light canopy pulsing for x/d ≤ 8. Stable to unstable (oscillations of ±7 deg) with medium to heavy canopy pulsing for x/d = 9.
		4.5	6	10	1.0	0.32	0.68	Very stable to stable (x/d = 9) with light (x/d ≤ 7) to medium (x/d ≥ 8) canopy pulsing. Fair (x/d = 6) to good inflation.
		5.0				0.27	0.55	Very stable to stable (x/d = 10). Light canopy pulsing increasing to medium to heavy at x/d = 10. Good inflation for x/d < 10.
		5.5				0.21	0.49	Very stable at all x/d values. Fair (x/d = 6) to good inflation. Light canopy pulsing for x/d > 7.
		6.0				0.21	0.42	Very stable and well inflated at all x/d values. Light to medium (x/d = 10) canopy pulsing.
	2	2.0	4	7	1.0	0.88	1.18	Very stable and well inflated at all x/d values. Little or no canopy pulsing.
		2.5				0.85	1.04	Same as M_∞ = 2.0

TABLE I (Continued)

Parachute Config.	Forebody Config.	M_∞ (Nominal)	x/d		q_∞, psia	C_{D_p}		Remarks
			Min.	Max.		Min.	Max.	
2	2	3.0	4	7	1.0	0.73	0.89	Same as M_∞ = 2.
		3.5				0.66	0.77	Very stable and well inflated at all x/d values. Very light canopy pulsing with periods of medium, rapid pulsing at x/d = 7.
		4.0			0.5	0.72	0.81	Very stable and well inflated at all x/d values. Light canopy pulsing at x/d = 7.
					1.0	0.64	0.72	Same as M_∞ = 3.5; q_∞ = 1.0.
					1.5	0.56	0.67	Very stable and well inflated with light canopy pulsing at all x/d values.
		4.5			1.0	0.61	0.69	Very stable and well inflated at all x/d values, with light rapid canopy pulsing at x/d > 4.
		5.0				0.44	0.61	Very stable and well inflated at all x/d values. Light rapid canopy pulsing increasing to medium at x/d = 7. Slowly rolling back and forth at x/d = 4.
		5.5				0.39	0.57	Very stable and well inflated at all x/d values. Light to medium rapid canopy pulsing at all x/d values.
		6.0				0.28	0.51	Same as M_∞ = 5.5.

TABLE I (Concluded)

Parachute Config.	Forebody Config.	M_∞ (Nominal)	x/d		q_∞, psia	C_{D_p}		Remarks
			Min.	Max.		Min.	Max.	
2	3	3.0	3	6	1.0	0.65	1.02	Very stable at all x/d values. Fair to poor inflation at x/d = 3, good inflation for x/d > 3. No canopy pulsing for x/d < 6. Light canopy pulsing at x/d = 6 with intermittent medium to heavy pulsing.
		3.5	3	5		0.33	0.96	Same as M_∞ = 3 except no canopy pulsing.
		4.0	3	6	0.5	0.20	0.79	Very stable at all x/d values. Poor inflation at x/d = 3, increasing to fair at x/d = 4 and good at x/d > 4.
			3	5	1.0	0.30	0.82	Same as q_∞ = 0.5 except good inflation for x/d > 3.
			3	6	1.5	0.65	0.86	Very stable (x/d ≤ 4) to stable (x/d = 5 and 6). Good inflation at all x/d values. Light pulsing increasing to heavy at x/d = 5 and 6.
		4.5			1.0	0.25	0.75	Very stable (x/d ≤ 4) to stable (x/d ≥ 5). Poor inflation at x/d = 3, good inflation for x/d > 3. Medium to heavy canopy pulsing at all x/d values.
		5.0				0.20	0.65	Same as M_∞ = 4.5 except fair inflation at x/d = 4.
		5.5				0.17	0.54	Very stable (x/d ≤ 4) to stable (x/d ≥ 5). Poor (x/d ≤ 4) to fair (x/d = 5) to good (x/d = 6) inflation. Medium to heavy canopy pulsing at all x/d values.
		6.0				0.10	0.52	Same as M_∞ = 5.5.

DOCUMENT CONTROL DATA - R & D

(Security classification of title, body of abstract and indexing annotation must be entered when the overall report is classified)

1. ORIGINATING ACTIVITY *(Corporate author)* Arnold Engineering Development Center ARO, Inc., Operating Contractor Arnold Air Force Station, Tennessee	2a. REPORT SECURITY CLASSIFICATION UNCLASSIFIED 2b. GROUP N/A

3. REPORT TITLE

THE DRAG AND PERFORMANCE CHARACTERISTICS OF FLEXIBLE SUPERSONIC DECELERATOR MODELS AT MACH NUMBERS FROM 2 TO 6

4. DESCRIPTIVE NOTES *(Type of report and inclusive dates)*

Final Report September 12 to 16, 1967

5. AUTHOR(S) *(First name, middle initial, last name)*

A. W. Myers, ARO, Inc.

6. REPORT DATE November 1967	7a. TOTAL NO. OF PAGES 27	7b. NO. OF REFS 3
8a. CONTRACT OR GRANT NO. AF 40(600)-1200 b. PROJECT NO 6065 c. Program Element 6240533F d. Task 606507	9a. ORIGINATOR'S REPORT NUMBER(S) AEDC-TR-67-224 9b. OTHER REPORT NO(S) *(Any other numbers that may be assigned this report)* N/A	

10. DISTRIBUTION STATEMENT

Subject to special export controls; transmittal to foreign governments or foreign nationals requires approval of Air Force Flight Dynamics Laboratory (FDFR), Wright-Patterson AFB, Ohio.

11. SUPPLEMENTARY NOTES Available in DDC.	12. SPONSORING MILITARY ACTIVITY Air Force Flight Dynamics Laboratory Air Force Systems Command Wright-Patterson AFB, Ohio

13. ABSTRACT

The drag and stability characteristics of flexible supersonic decelerator models at various positions aft of double-strut mounted forebodies were investigated in the 40-in. supersonic tunnel of the von Kármán Gas Dynamics Facility. Data were obtained at Mach numbers from 2 to 6 at dynamic pressures corresponding to pressure altitudes which ranged from 94,000 to 153,000 ft. Selected typical results are presented.

This document is subject to special export controls and each transmittal to foreign governments or foreign nationals may be made only with prior approval of Air Force Flight Dynamics Laboratory (FDFR), Wright-Patterson AFB, Ohio.

14. KEY WORDS	LINK A		LINK B		LINK C	
	ROLE	WT	ROLE	WT	ROLE	WT
parachutes						
decelerators						
drag measurements						
performance characteristics						
supersonic flow						
hypersonic flow						